Benchmarking geant4 nuclear models for hadron therapy with 95 MeV/nucleon carbon ions

J. Dudouet, D. Cussol, D. Dominique Durand, M. Labalme

Benchmarking GEANT4 nuclear models for carbon-therapy at 95 MeV/A

J. Dudouet, D. Cussol, D. Durand and M. Labalme

LPC Caen, ENSICAEN, Université de Caen, CNRS/IN2P3, Caen, France

Abstract.

In carbon-therapy, the interaction of the incoming beam with human tissues may lead to the production of a large amount of nuclear fragments and secondary light particles. An accurate estimation of the biological dose deposited into the tumor and the surrounding healthy tissues thus requires sophisticated simulation tools based on nuclear reaction models. The validity of such models requires intensive comparisons with as many sets of experimental data as possible. Up to now, a rather limited set of double differential carbon fragmentation cross sections have been measured in the energy range used in hadrontherapy (up to 400 MeV/A). However, new data have been recently obtained at intermediate energy (95 MeV/A). The aim of this work is to compare the reaction models embedded in the GEANT4 Monte Carlo toolkit with these new data. The strengths and weaknesses of each tested model, i.e. G4BinaryLightIonReaction, G4QMDReaction and INCL++, coupled to two different de-excitation models, i.e. the generalized evaporation model and the Fermi break-up are discussed.

PACS numbers: 25.70.Mn, 25.70.-z,24.10.Lx,

Submitted to: *Phys. Med. Biol.*

1. Introduction

The use of carbon ions in oncology is motivated by some specific advantages such as a limited straggling effect (small angular scattering) and a high dose deposition at the end of the radiation range (i.e. at the Bragg peak). Moreover, the biological efficiency, which is strongly correlated to the linear energy transfer (LET), is larger in the Bragg peak region as compared to protons. Carbon ions allow thus to better target the tumor while preserving the surrounding healthy tissues. However, the physical dose deposition is affected by the inelastic processes of the ions along the penetration path in human tissues (Schardt et al. 1996, Matsufuji et al. 2003). For instance, the number of incident ions reaching the tumor (at the Bragg peak depth) is reduced up to 70% for 400 MeV/A ^{12}C in tissue equivalent material (Haettner et al. 2006). Carbon beam fragmentation in human body leads to the production of secondary lighter fragments with larger ranges and larger angular spreadings. Such fragments have thus different relative biological effectivenesses (RBE) in the contribution of the deposited dose. These effects, due to carbon fragmentation, result in a more complex spatial dose distribution, particularly on healthy tissues, as compared with protons for instance.

In view of the previous remarks, to keep the benefits of carbon ions in radiotherapy requires a very high accuracy on the dose deposition pattern ($\pm$3% on the dose value and $\pm$1 mm spatial resolution). In planning a tumor treatment, the fragmentation processes need to be correctly evaluated to compute the biological dose all along the beam path. Monte Carlo methods are probably the most powerful tools to take into account such effects. Even though they generally cannot be directly used in treatment planning system (TPS) because of a too long processing time, they can be used to constrain and optimize analytical TPS (Sihver & Mancusi 2009, Krämer & Durante 2010) or to generate complete and accurate data bases.

The ability of FLUKA (Battistoni et al. 2007) and GEANT4 (Agostinelli et al. 2003) Monte Carlo codes to reproduce carbon fragmentation has been recently studied. Results obtained at 95 MeV/A ^{12}C on thick PMMA targets (Braunn et al. 2011) have shown discrepancies up to one order of magnitude as compared to experimental data. The same difficulties for Monte Carlo models to reproduce data have been observed on thick water and polycarbonate targets for ^{12}C beams in the energy range from 100 to 500 MeV/A (Böhlen et al. 2010) and for 62 MeV/A ^{12}C on thin carbon target (de Napoli et al. 2012).

A new set of double differential cross section data have been recently obtained by our collaboration (Dudouet et al. 2013*b*). These data provide good quality measurements of 95 MeV/A ^{12}C fragmentation on thin targets (C, CH_2, Al, Al_2O_3, Ti and PMMA). These experimental data are used in this work to test the different nuclear models embedded in the GEANT4 framework and used in hadrontherapy studies. These nuclear models are: G4BinaryLightIonReaction (BIC), G4QMDReaction (QMD) and INCL++. They are coupled to two de-excitation after-burners: the generalized evaporation model (GEM) and the Fermi break-up (FBU). Strengths and weaknesses of these different models in

reproducing the fragment production yields, the angular and energy distributions, as well as the target mass dependence will be discussed.

2. Methods

GEANT4 is a Monte Carlo particle transport code developed at CERN. It is used to simulate the propagation of particles through matter by taking into account both electromagnetic and nuclear processes. It is widely used in a variety of application domains, including medical physics. The 9.6 version of GEANT4 has been used in this work. Electromagnetic interactions are those developed in the "electromagnetic standard package option 3". Particle transport cuts have been set to 700 μm. Total nucleus-nucleus reaction cross sections have been determined using the recently implemented Glauber-Gribov model (Grichine 2009). This model provides the full set of nucleus-nucleus cross-sections needed for the GEANT4 tracking (inelastic, elastic, particle production and quasi-elastic) for all incident energies above 100 keV/A.

Nuclear reactions are usually described by a two-step process: a first dynamical step called "entrance channel" followed by an after-burner step called "exit channel". The entrance channel model describes the collision and the production of excited nuclear species until thermal equilibrium is achieved. The decay of such hot species is thus considered in a second step by means of statistical after-burner models. All nuclear models implemented in GEANT4 follow this scheme. In this work, three different entrance channel models are coupled with two exit channel models leading to six different combinations.

2.1. The GEANT4 entrance channel models

Two nuclear models are currently recommended to perform simulations for hadron therapy. The first one is a binary intra-nuclear cascade (BIC) called G4BinaryLightIonReaction (Geant4 2012). This is an extension of the Binary Cascade model (Folger et al. 2004) for light ion reactions. This model can be characterized as an hybrid model between a classical cascade code and a quantum molecular dynamics (QMD) description because the 'participating' particles are described by means of gaussian wave functions. By 'participating' particles, it is meant those particles that are either primary particles from the projectile or particles generated and/or scattered during the cascade process. The Hamiltonian is built with a time-independent optical potential taking into account only the 'participants'. Note that in this model, scattering between participants is not taken into account. Participants are tracked until escaping from the nucleus or until the end of the cascade. The cascade stops if the mean kinetic energy of participants in the system is below 15 MeV or if all the participant kinetic energies are below 75 MeV. If such conditions are fulfilled, the system is assumed to have reached thermal equilibrium.

An other model used in hadron therapy is a QMD-like model called

G4QMDReaction (Koi 2010) adapted from the JAERI QMD (JQMD) code (Niita et al. 1995, Niita et al. 1999). As for the BIC model, the basic assumption of a QMD model is that each nucleon is decribed by a gaussian wave function which is propagated inside the nuclear medium. At variance with the previous model, in G4QMDReaction, all nucleons of the target and of the projectile are taken into account. Each nucleon is thus considered as 'participant'. The particles are propagated and interact by means of a phenomenological nucleon-nucleon potential. The time evolution of the system is stopped at 100 fm/c where it is assumed that equilibrium has been achieved.

A third model has been used in this work: the Liège Intranuclear Cascade model INCL++ (Boudard et al. 2013, Kaitaniemi et al. 2011, Geant4 2012). The last version implemented in GEANT4 is labeled as INCL++ v5.1.8. This model has recently shown promising results (Braunn et al. 2013) comparable with the BIC or QMD models. Nucleons are modeled as a free Fermi gas in a static potential well. To treat the collision, a target volume is calculated for each impact parameter. This volume is used to label nucleons as spectators or participants. All nucleons from the target, and nucleons from the projectile inside the target volume are considered as participants. Only collisions where participants are involved are then taken into account. The nucleus-nucleus collision is thus not treated symmetrically. Results have shown that INCL better reproduces the target fragmentation than the projectile fragmentation (Braunn et al. 2013). In view of this, INCL treats by default the collision in inverse kinematics (target impinging on projectile), in order to obtain the best reproduction of the projectile fragmentation. However, INCL is not able to use projectile heavier than A=18. If the target is heavier than A=18, the collision will then be performed in direct kinematics. If both target and projectile are heavier than A=18, the description of the collision uses the G4BinaryLightIonReaction model. This asymmetry in the treatment of the projectile and the target and the discontinuity at mass 18 is at the origin of some problems that will be discussed later. The cascade is stopped when no participants are left in the nucleus or when a stopping time defined as : $t_{\mathrm{stop}} = 70 \times (A_{\mathrm{target}}/208)^{0.16}$ fm/c is reached.

For all models, clustering of the nucleons in phase-space is considered to produce excited species at the end of the cascade. The excitation energy of each species is then estimated and is the input for the de-excitation process considered in the statistical after-burner codes.

2.2. The GEANT4 exit channel models

GEANT4 provides several de-excitation (after-burner) models which have been recently improved (Quesada et al. 2011). These models describe particle evaporation from excited nuclear species produced in the entrance channel. Two models have been considered in this work.

The first one is the generalized evaporation model (GEM) (Furihata 2000, Geant4 2012). Based on the Weisskopf-Ewing evaporation model (Weisskopf & Ewing 1940), it

considers sequential particle emission up to ^{28}Mg as well as fission and gamma decay.

The second model is the Fermi Break-up model (Geant4 2012). This model considers the decay of an excited nucleus into n stable fragments produced in their ground state or in low-lying discrete states. The break-up probabilities for each decay channel are first calculated by considering the n-body phase space distribution. Such probabilities are then used to sample the decay channels by a Monte-Carlo procedure. This model is only used for light nuclei (Z≤8 and A≤16). For heavier nuclei, the de-excitation process is considered using the GEM model.

3. Results

The results of the models considered above are now compared with data obtained during the E600 experiment performed in May 2011 at the GANIL facility. The experiment has allowed to measure the double differential cross sections of various species in 95 MeV/A ^{12}C reactions on H, C, O, Al and ^{nat}Ti targets (Dudouet et al. 2013*a*, Dudouet et al. 2013*b*). These data are available with free access on the following web-site `http://hadrontherapy-data.in2p3.fr`. We first consider a comparison of simulated production cross sections (angular and energy distributions) with the experimental data in the case of a carbon target. Then, the target mass dependence will be studied.

For a realistic comparison, the energy thresholds and the geometry of the experiment have been implemented in the simulations.

3.1. A specific reaction mechanism: the participant-spectator model

Some characteristics of the results will be discussed in the framework of the participant-spectator picture of the collision (see for instance figure 1 (Durand et al. 2001, Babinet 1985)).

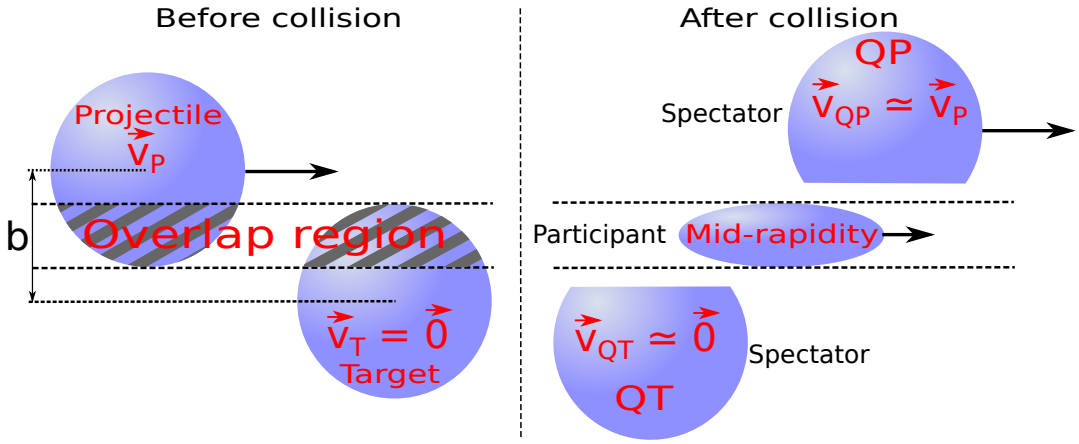

Figure 1. Schematic representation of the geometrical participant-spectator model in the laboratory frame.

This is a typical high energy process (in the GeV/A range) in which the internal velocities of the nucleons are (much) smaller than the relative velocity between the two partners of the reactions. However, recent analysis have shown that it could still be valid around 100 MeV/A incident energy (Dudouet et al. 2013*b*). In such a picture, for a finite impact parameter, b, those nucleons which are located in real space in the overlapping region of the two nuclei constitute the 'participants'. At variance, those nucleons of the projectile outside the overlapping region constitute the moderately excited quasi-projectile moving with a velocity close to the beam velocity. The same argument applies for the target. The participants constitute the so-called highly excited mid-rapidity source. The decay products from this source show an energy distribution shifted towards lower values as compared to the beam energy. Therefore, in such a picture, three energy contributions in the laboratory frame are expected: a first one close to the beam energy, a second one associated with the target at energies close to 0 and in between, a contribution associated with the participants. This latter is thus to a large extent strongly coupled to the size of the projectile and of the target and should show up as the size of the target increases.

3.2. Production cross sections

Figure 2 displays the production cross sections of the most abundant reaction products in the case of a carbon target. They are compared with the GEANT4 results with the different combinations between the entrance and exit channel models discussed previously. Note that the production cross section of ^{12}C fragments takes into account only inelastic interactions, excluding elastic scattering.

All in all, the results of Figure 2 clearly shows that none of the model combination is able to accurately reproduce the production rates. Moreover, it is not easy to identify which model combination is the most suited for a comparison with experimental data. However, it may be concluded that the influence of the entrance channel is larger than the influence of the exit channel model. Regarding the two exit channel models, the Fermi Break-up model seems, for a given entrance channel model, to be, in most cases, more compatible with the data. This was already mentioned in Böhlen et al. (2010) and Ivanchenko et al. (2012). This is due, to some extent, to the fact that the Fermi Break-up description allows to explore more available phase space (especially at high excitation energies for which three (or more) body decay may play an increasing role) than the GEM model for which only sequential evaporation is taken into account. In the following, we only consider calculations in which the Fermi Break-up model is used for the exit channel part.

3.3. Angular distributions

The E600 experimental setup allowed to cover an angular range from from 4° to 43° by steps of two degrees. Figure 3 displays the absolute angular cross-sections for carbon

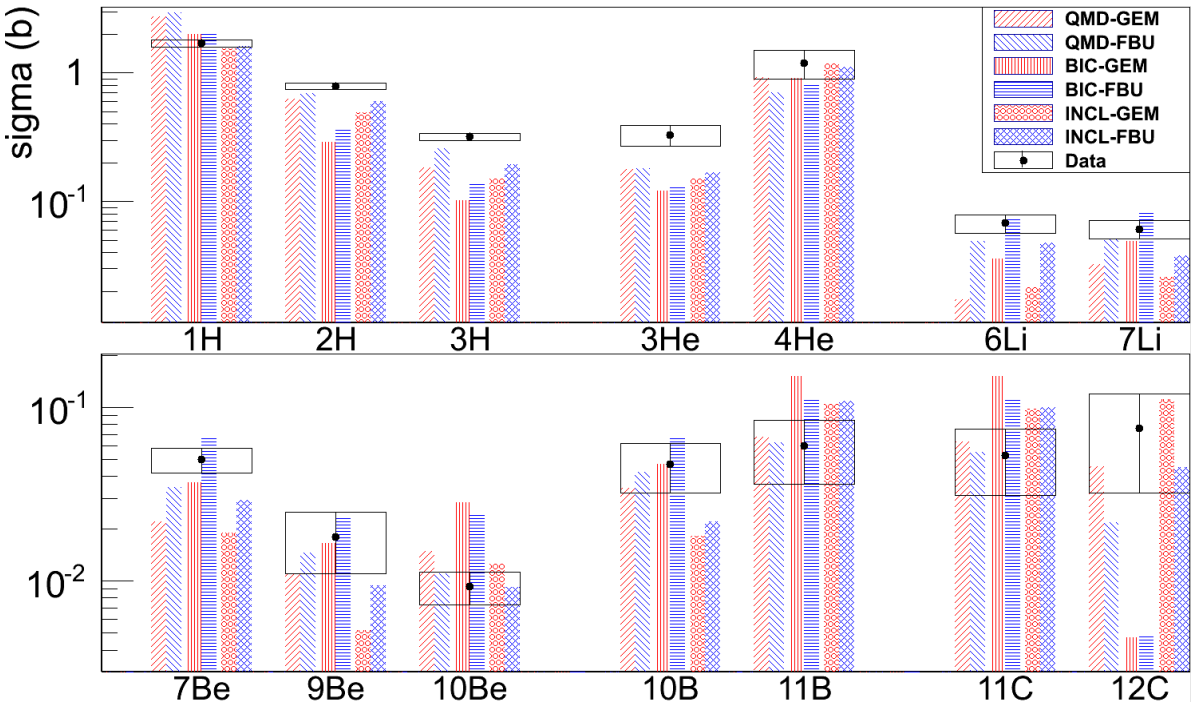

Figure 2. Comparisons between data and the different combination of entrance and exit channel models (see text) for the production cross sections of various isotopes in 95 MeV/A $^{12}C \rightarrow {}^{12}C$ reactions.

target for various species for both experimental data and for simulations using QMD, BIC, and INCL models coupled with the Fermi Break-up de-excitation model.

Although QMD is the most achieved model as far the dynamics of the collision is concerned, it fails to reproduce the angular distributions. It strongly overestimates the proton production (as also observed in figure 2), and poorly reproduces the three heavier isotopes considered here. The maximum values of the distributions are around 7° (apart for protons) with a fall off towards 0°. This is at variance with the experimental distributions showing an increase at very low angles.

The distributions obtained with the BIC model are slightly closer to the data as compared with QMD, especially at forward angles and for heavier fragment distributions (^{6}Li and ^{7}Be). The lack of α at forward angles may possibly come from a failure of the model to take into account the ^{12}C three alpha cluster structure. The global shape is however not correct. The quasi-projectile contribution is too large and the large angles are poorly reproduced. The angular distributions obtained with the BIC model increases around 25° (except for protons). This probably comes from the quasi-target contribution but is in disagreement with experimental data.

Finally, INCL is the model that seems to better reproduce the angular distributions, especially for light fragments. The shapes of protons and α distributions are nearly reproduced over the whole angular range, despite a small underestimation of the protons at forward angles. Regarding the ^{6}Li and ^{7}Be distributions, as for the BIC model, only the forward angles are well described. There remains problems at large angles where

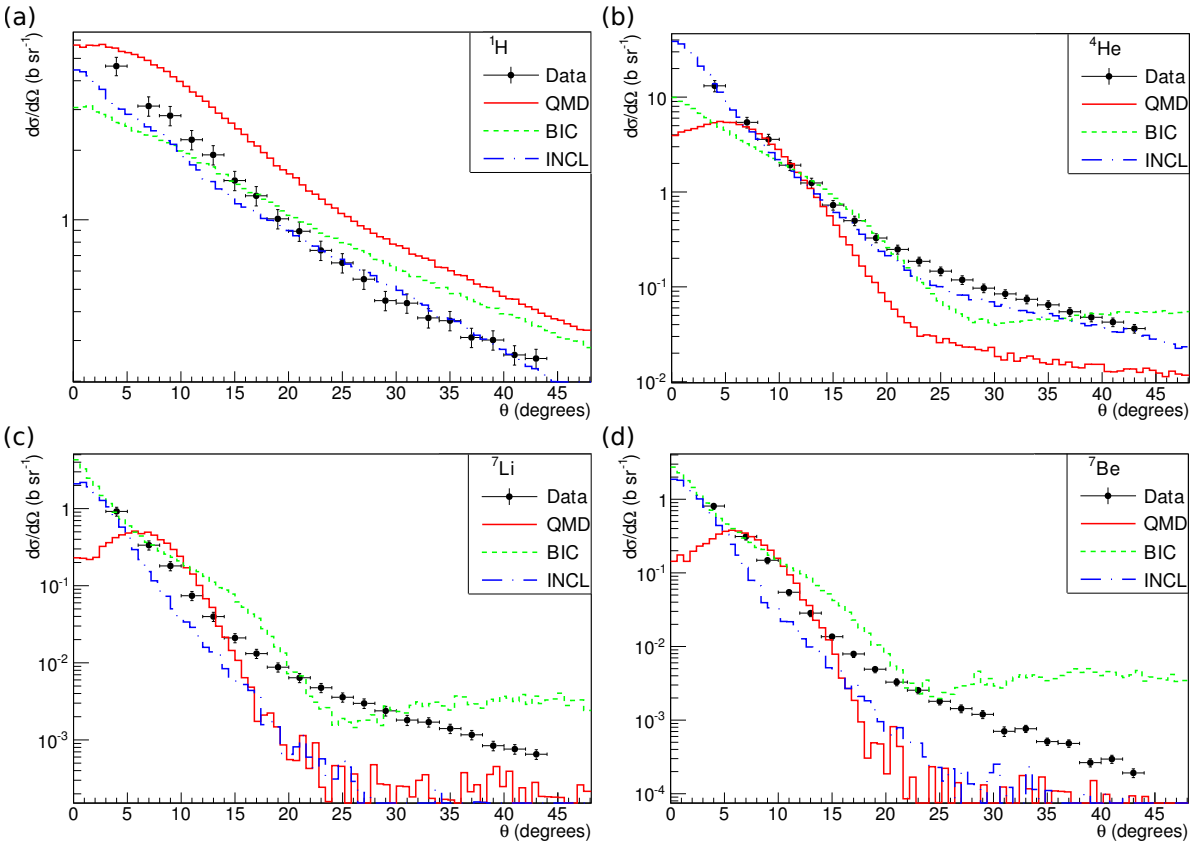

Figure 3. Absolute differential angular cross-sections of protons, ^{4}He, ^{6}Li and ^{7}Be. Experimental data: black points. Histograms: GEANT4 simulations with QMD, BIC and INCL models coupled to the Fermi Break-up de-excitation model as indicated in the insert.

the calculations strongly underestimate the data.

We have shown in Dudouet et al. (2013*b*) that the experimental angular distributions of particles emitted in the 95 MeV ^{12}C reaction on H, C, O, Al and ^{nat}Ti can be represented as the sum of a gaussian and an exponential contribution. None of the models used here are able to reproduce this trend. The main problem is associated with the inability of such models to reproduce the magnitude of the exponential contribution which is dominant at large angles. Since this contribution is mostly resulting from the mid-rapidity source discussed previously, it is tempting to conclude at this stage that the present models do not content the ingredients needed to describe the mid-rapidity processes. We now proceed with the energy distributions.

3.4. Energy distributions

The agreement with the double differential cross sections constitute the most severe test of the models. Figure 4 shows few examples of energy distributions obtained for ^{4}He and ^{7}Be at 4 and 17°.

Here, we would like to focus on the shape of the distributions rather than on

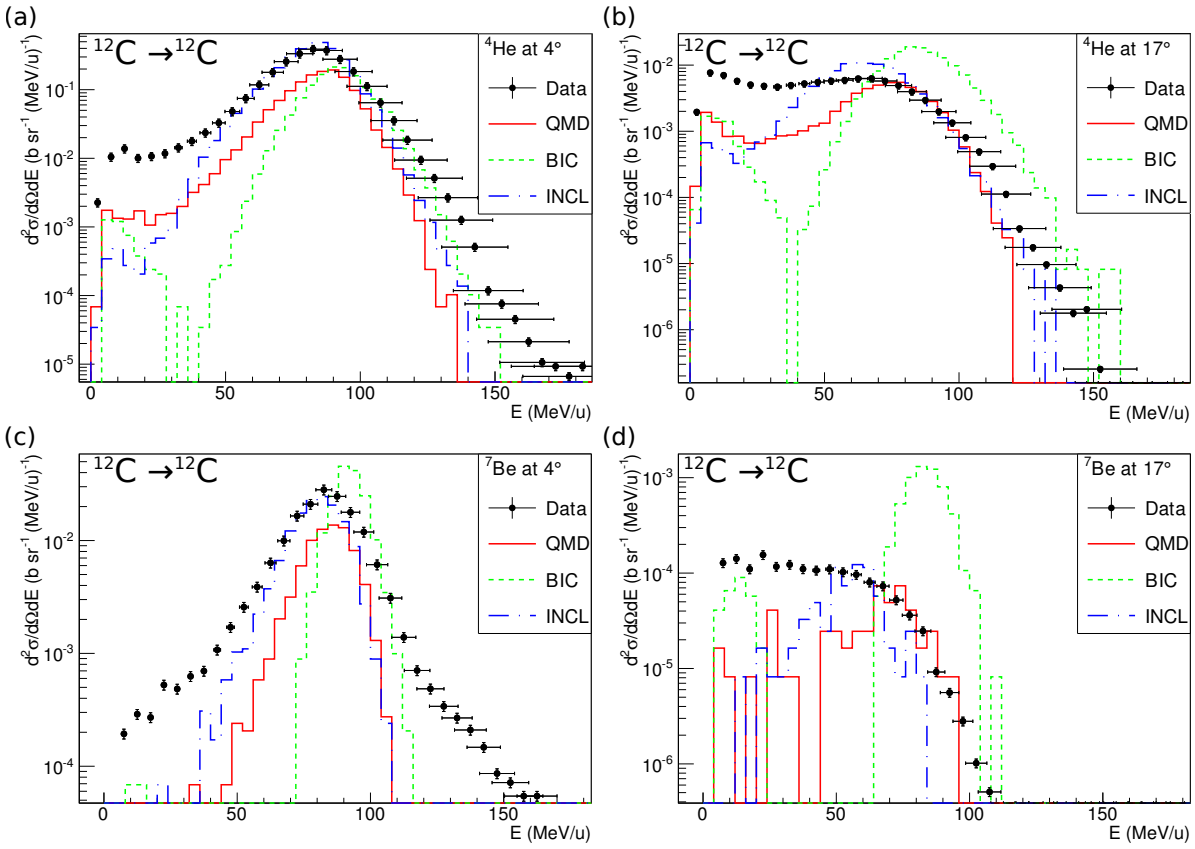

Figure 4. Energy distributions of ^{4}He and ^{7}Be fragments at 4 and 17°. Black points: experimental data. Histograms are for simulations with QMD, BIC and INCL models coupled to the Fermi Break-up de-excitation model (see insert).

the absolute magnitude. The distributions may be interpreted as follows: the major contribution originates from the decay of the quasi-projectile and is thus located at an energy close to the beam energy per nucleon. At larger angles, this contribution tends to vanish because of the strong focusing of the quasi-projectile. The low energy part of the distribution is associated with the species produced at mid-rapidity and also with the decay of the target-like although this last contribution becomes dominant only at very large angles and can be poorly detected due to threshold effects. Therefore, the ability of the models to reproduce the data can be appreciated on these two physical aspects: the decay of the projectile-like and the particle production mechanism at mid-rapidity.

Among the three models, BIC shows the strongest disagreement with the experimental data. In particular, the model is unable to account for the mid-rapidity contribution. This is due to the binary nature of the reaction mechanism assumed in the model. Moreover, the mean energy of the quasi-projectile contribution is too large as compared to data and its contribution remains too important at large angle. This leads for instance to the very strong disagreement shown in figure 4 (d) for ^{7}Be fragments at 17°.

The INCL model reproduces better the quasi projectile contribution both for the

mean and the width of the energy distribution. It also predicts more fragments at low energies (0 <E< 50 MeV/A) as compared to the BIC model. However, the results still underestimate the data. Moreover, the shape of the distributions at low energies (mid-rapidity contribution) is not in agreement with the data.

Contrary to angular distributions, the QMD model reproduces better the shape of the energy distributions. Although the mean energy of the quasi-projectile peak is slightly too high, the shape of the mid-rapidity contribution is better reproduced than for the BIC or INCL models. However, as for other models, it underestimates the mid-rapidity contribution.

The remarks mentioned above are valid for all fragments from protons to carbon isotopes. The main conclusion that can be drawn is that none of the tested models is able to reproduce simultaneously the quasi-projectile, the quasi-target and the mid-rapidity contributions. The INCL model better reproduces the quasi-projectile contribution: it is probably the best model for the description of the quasi-projectile. In contrast, the QMD model describes better the mid-rapidity emission, probably due to the fact that it is the only model to take into account the time propagation and the interaction of all the nucleons in the reaction. Similar conclusions have been drawn at lower energy in de Napoli et al. (2012), where the BIC and QMD models were tested in 62 MeV/A $^{12}C \rightarrow {}^{12}C$ induced reactions.

3.5. Results with other targets

Our experiment allowed to gather data for a series of targets ranging from hydrogen up to titanium. The target dependence on the double differential cross sections is now investigated. Figure 5 displays the α energy distributions at 4° for the hydrogen, oxygen, aluminum and titanium targets for both data and simulations using QMD, BIC and INCL models coupled to the Fermi Break-up de-excitation model.

The three models reproduce quite well the data for the hydrogen target, especially INCL. This result is not surprising in the sense that these models are mostly based on the concept of nuclear cascade which was originally dedicated to nucleon-nucleus collisions. In such reactions, the geometry of the collision is rather simple and the description of the quasi-projectile is easier than for nucleus-nucleus reactions. More, with the hydrogen target, the α is mainly produced by the quasi-projectile de-excitation. However, the experimental data exhibits a small contribution at low energy (below 50 MeV/A) and INCL is the only model to reproduce this contribution.

Nevertheless, the heavier the target, the larger the disagreement between the simulations and the experimental data. From carbon to titanium, the three models reproduce quite well the quasi-target and the quasi-projectile contributions. The difficulty to produce mid-rapidity fragments is evidenced. The discrepancy is amplified as the target mass increases emphasizing the increasing role of mid-rapidity in the data as a simple consequence of the geometry of the reaction. The larger the mass of the target, the larger the size of the mid-rapidity region. The BIC model does not produce

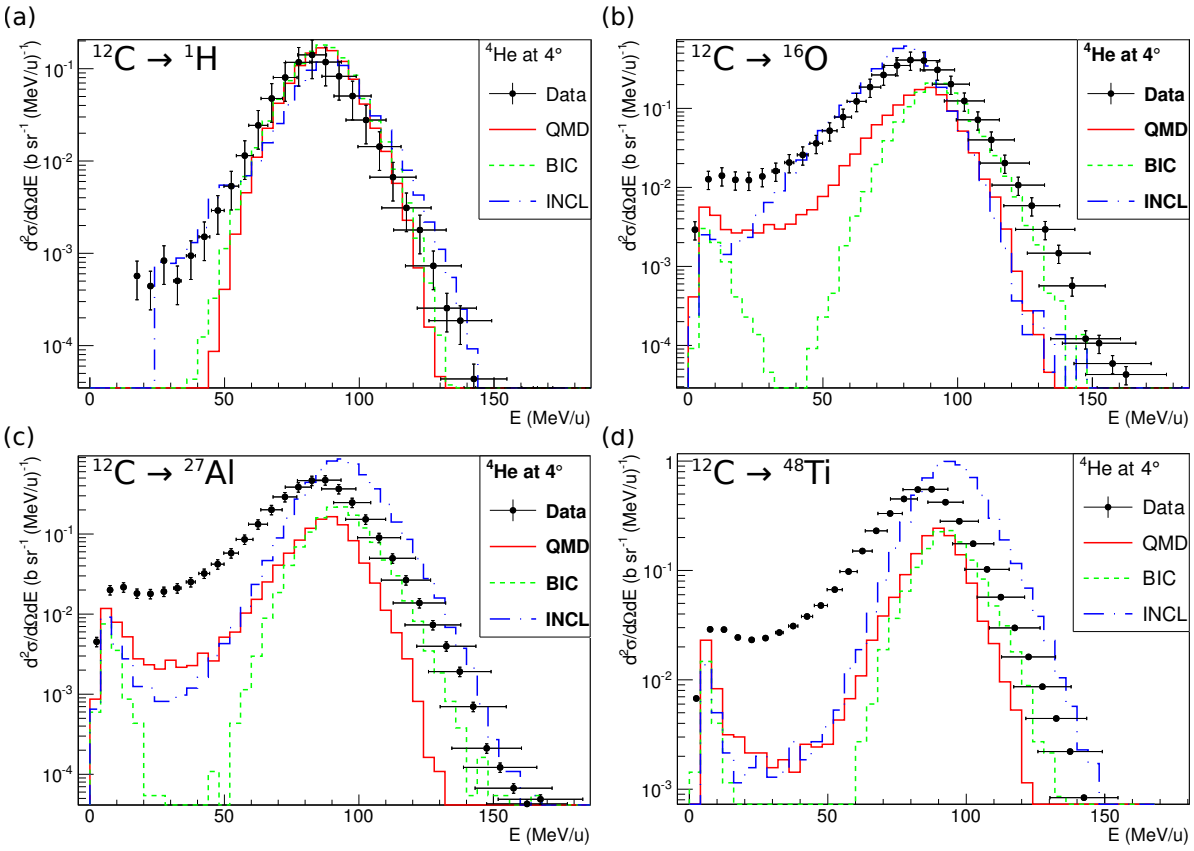

Figure 5. Energy distributions of α particles at 4° for hydrogen (a), oxygen (b), aluminum (c) and titanium (d) targets. Black points: experimental data. Histograms: simulations (see insert).

mid-rapidity fragments (around E = 40-50 MeV/A) as expected. Although the situation is slightly better for INCL or QMD models, there is clearly something missing in these models.

A particular attention needs to be paid to the INCL model. For the aluminum and titanium targets, the shape of the energy distribution changes with respect to lighter targets. The projectile contribution is overestimated and the mean energy is too large. The reason is due to the discontinuity in the treatment of the kinematics when the target is larger than A=18 as mentioned in section 2.1. Otherwise, for lighter targets, results concerning the quasi-projectile are promising while the production at mid-rapidity remains underestimated.

In the participant-spectator reaction mechanism, the mid-rapidity contribution originates from the overlap region as already mentioned previously. This is thus a geometrical contribution, which increases significantly with the target size, as it is observed experimentally when going from the hydrogen to the titanium target: more and more fragments are produced in the low energy region. The three models that have been used here fail in accurately reproducing this region and the discrepancy increases with the mass of the target. This may be due to the fact that none of them take

accurately into account the possibility to produce sizeable clusters in the overlapping region. This point should deserve additional studies.

4. Conclusions

In this work, for the purpose of hadrontherapy studies, comparisons have been performed between experimental data collected in 95 MeV/A ^{12}C reactions on H, C, O, Al and ^{nat}Ti targets and GEANT4 simulations in order to test the models embedded in the GEANT4 nuclear reaction package. The G4BinaryLightIonReaction (BIC), the G4QMDReaction (QMD) and the INCL++ (INCL) entrance channel models have been coupled to the generalized evaporation model (GEM) and the Fermi break-up model (FBU) exit channel models.

The main conclusion is that up to now, none of these six models combinations is able to accurately reproduce the data, neither in term of production rates nor for angular or energy distributions.

This study has shown that the entrance channel model characteristics have a larger effect on particles and fragments production as compared to the choice of the exit channel description. However, the Fermi break-up de-excitation model seems to give better results than the generalized evaporation model.

As for angular distributions, apart from INCL which reproduces quite well protons (with a small disagreement at forward angles) and α distributions for the carbon target, the models are not able to reproduce the data. The QMD model is the worst, with a maximum value of the distribution at around 7° and an unexpected fall off towards 0°.

On the contrary, QMD is the one which better reproduces the energy distributions for all considered fragments. Apart from the hydrogen target, the BIC model fails to reproduce the data and in particular, it does not produce particles at low energy. The INCL model reproduces very well the quasi-projectile contribution if the target is not larger than A=18.

Finally, a study of the target mass dependence shows that the three models do not succeed in reproducing realistically the production of species at mid-rapidity. Comparisons with a simple phenomenological model that takes into account the geometrical overlap region is planned in a near future.

References

Agostinelli S et al. 2003 *Nucl. Instrum. Methods A* **506**, 250 – 303.

Babinet R 1985 *Collisions entre ions lourds à haute énergie - Approche expérimentale* École Joliot-Curie de Physique Nucélaire.

Battistoni G, Cerutti F, Fass A, Ferrari2 A, Muraro S, Ranft J, Roesler S & Sala P R 2007 *AIP Conference Proceedings* **896**, 31–49.

Böhlen T T, Cerutti F, Dosanjh M, Ferrari A, Gudowska I, Mairani A & Quesada J M 2010 *Phys. Med. Biol.* **55**, 5833.

Boudard A, Cugnon J, David J, Leray S & Mancusi D 2013 *Phys. Rev. C* **87**, 014606.

Braunn B, Boudard A, Colin J, Cugnon J, Cussol D, David J C, Kaitaniemi P, Labalme M, Leray S & Mancusi D 2013 *J. Physique: Conference Series* **420**(1), 012163.

Braunn B et al. 2011 *Nucl. Instrum. Methods B* **269**, 2676–2684.

de Napoli M et al. 2012 *Phys. Med. Biol.* **57**, 7651–767.

Dudouet J et al. 2013*a* *Nucl. Instrum. Methods A* **715**(0), 98 – 104.

Dudouet J et al. 2013*b* *Phys. Rev. C* **88**, 024606.

Durand D, Suraud E & Tamain B 2001 *Nuclear Dynamics In The Nucleonic Regime* Series in fundamental and applied nuclear physics.

Folger G, Ivanchenko V & Wellisch J 2004 *Eur. J. Phys. A* **21**(3), 407–417.

Furihata S 2000 *Nucl. Instrum. Methods B* **171**(3), 251–258.

Geant4 2012 *Geant4 Physics Reference Manual* (Version 9.6.0), Chapters 30, 33, 34, 36 and 38.

Grichine V 2009 *Eur. J. Phys. C* **62**(2), 399–404.

Haettner E, Iwaseand H & Schardt D 2006 *Rad. Prot. Dosim.* **122**, 485–487.

Ivanchenko A V, Ivanchenko V N, Quesada J M & Incerti S 2012 *International Journal of Radiation Biology* **88**(1-2), 171–175.

Kaitaniemi P, Boudard A, Leray S, Cugnon J & Mancusi D 2011 *in* 'Progress in NUCLEAR SCIENCE and TECHNOLOGY' Vol. 2 pp. 788–793.

Koi T 2010 *in* 'Proceedings of the MC2010 Monte Carlo Conference'.

Krämer M & Durante M 2010 *Eur. J. Phys. D* **60**(1), 195–202.

Matsufuji N, Fukumura A, Komori M, Kanai T & Kohno T 2003 *Phys. Med. Biol.* **48**, 1605–1623.

Niita K, Chiba S, Maruyama T, Maruyama T, Takada H, Fukahori T, Nakahara Y & Iwamoto A 1995 *Phys. Rev. C* **52**, 2620–2635.

Niita K, Chiba S, Maruyama T, Maruyama T, Takada H, Fukahori T, Nakahara Y & Iwamoto A 1999 *JAERI-Data/Code 99-042* .

Quesada J M, Ivanchenko V, Ivanchenko A, Cortés-Giraldo M A, Folger G, Howard A & Wright D 2011 *in* 'Progress in NUCLEAR SCIENCE and TECHNOLOGY' Vol. 2 pp. 936–941.

Schardt D et al. 1996 *Adv. Space Res.* **17**, 87–94.

Sihver L & Mancusi D 2009 *Rad. Meas.* **44**(1), 38 – 46.

Weisskopf V F & Ewing D H 1940 *Phys. Rev.* **57**, 472–485.